JOURNAL OF PETROLOGY | VOLUME 51 | NUMBERS 1 & 2 | PAGES 43–53 | 2010 | doi:10.1093/petrology/egp057

Microstructural and Rheological Evolution of a Mantle Shear Zone

PHILIP SKEMER[1]*, JESSICA M. WARREN[2], PETER B. KELEMEN[3] AND GREG HIRTH[1]

[1]DEPARTMENT OF GEOSCIENCES, BROWN UNIVERSITY, PROVIDENCE, RI 02912, USA

[2]DEPARTMENT OF TERRESTRIAL MAGNETISM, CARNEGIE INSTITUTION, WASHINGTON, DC 20015, USA

[3]LAMONT–DOHERTY EARTH OBSERVATORY, COLUMBIA UNIVERSITY, PALISADES, NY 10964, USA

RECEIVED JANUARY 24, 2008; ACCEPTED AUGUST 4, 2009
ADVANCE ACCESS PUBLICATION OCTOBER 7, 2009

We conducted a microstructural study of a high-strain mantle shear zone from the Josephine Peridotite, SW Oregon, USA. The goal of this study is to understand how microstructural evolution at large strains leads to transitions in rheological behavior. The shear zone we investigated exhibits higher strain and greater localization than previously studied shear zones in the Josephine Peridotite. The margins of the shear zone have a homogeneous microstructure, characterized by moderately strong olivine fabrics, fairly weak orthopyroxene fabrics, and grain sizes of 2–3 mm. The highly deformed samples from the center of the shear zone display two distinct microstructural domains—a relatively coarse-grained domain (~550 μm) that contains only olivine and a finer-grained domain (~250 μm) that contains both olivine and orthopyroxene. The coarse-grained domain has a strong E-type olivine lattice-preferred orientation (LPO). Within the fine-grained domain the olivine LPO is also E-type, but significantly weaker. The E-type fabrics are rotated slightly past the shear plane, providing the first field-based confirmation of similar experimental observations. The presence of E-type fabrics, which form in the presence of moderate quantities of water, also highlights the potential importance of water to shear zone evolution. The orthopyroxene in the fine-grained domains has no LPO, suggesting that a transition to grain-size sensitive deformation occurred. The microstructural transition in orthopyroxene may have resulted in a marked weakening of the rock, suggesting that orthopyroxene plays a critical role in shear localization. These samples provide a crucial microstructural link between moderately localized shear zones and highly deformed ultramylonites.

KEY WORDS: *olivine; orthopyroxene; mylonite; Josephine; LPO*

INTRODUCTION

We investigated a ductile shear zone from the Fresno Bench section of the Josephine Peridotite, SW Oregon, USA (Kelemen & Dick, 1995) (Fig. 1). This shear zone is of particular interest because it exhibits a high degree of localization in comparison with other shear zones within the Josephine Peridotite. Its microstructures preserve a complex deformation history that provides new constraints on the initiation, evolution, and rheology of mantle shear zones.

Ductile shear zones are common features of ophiolitic and orogenic peridotites, where localized deformation occurs on a variety of length scales. They display a range of strain histories and deformation microstructures, from moderately deformed tectonites with relatively coarse, equant grains, to highly deformed ultramylonites with fine-grained, banded microstructures (White *et al.*, 1980; Drury *et al.*, 1991). Shear zones are of considerable interest because localized deformation is thought to be essential for the generation of Earth-like plate tectonics (Bercovici & Karato, 2002; Bercovici, 2003). However, details of the microphysical processes that produce localized deformation are still poorly understood.

In many cases, localization has been attributed to a reduction in grain size and an associated transition from dislocation creep to grain-size sensitive creep (Rutter & Brodie, 1988; Drury *et al.*, 1991). Grain-size reduction in mantle shear zones may be promoted by the fluxing of a reactive melt (Dijkstra *et al.*, 2002), metamorphic reactions (Newman *et al.*, 1999), deformation-induced dynamic

*Corresponding author. Telephone: 401-863-1044.
E-mail: philip.skemer@brown.edu

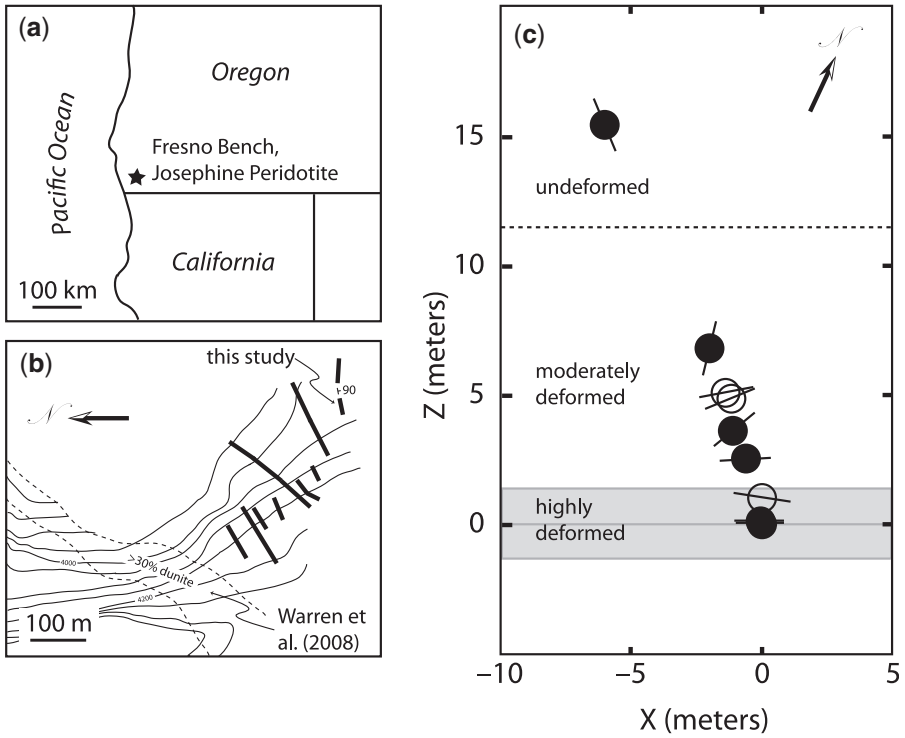

Fig. 1. (a) Regional map showing the location of the Fresno Bench section of the Josephine Peridotite. (b) Map of the southern portion of the Fresno Bench, modified from Kelemen & Dick (1995). Fine lines are 50 foot elevation contours. The bold lines are shear zones identified by Kelemen & Dick; the shear zone investigated here is on the southernmost tip of Fresno Bench. The dashed lines outline a region with >30% dunite, which contains the shear zone documented by Warren *et al.* (2008). (c) Sample location map projected into the structural X–Z plane. Filled circles indicate samples investigated in this study. The short black lines through each circle show the orientation of associated pyroxenite bands, and thus represent the magnitude of shear strain. The center of the shear zone is marked by a gray line. The gray band delineates the highly deformed core of the shear zone. The dashed line indicates the approximate location of the outer boundary of the shear zone. The region between the gray band and the dashed line is the moderately deformed margin of the shear zone.

recrystallization (Drury *et al.*, 1991) or cataclasis (Vissers *et al.*, 1997). However, the magnitude of weakening is often difficult to ascertain. This is particularly true in cases where orthopyroxene plays a critical role in rheology, as the lack of experimental data hinders our ability to study shear zone rheology quantitatively. None the less, it has become increasingly apparent that the recrystallization of orthopyroxene is necessary to induce a transition to grain-size sensitive creep, either through its own intrinsic rheological behavior (Skemer & Karato, 2008) or indirectly through its effect on olivine grain size (e.g. Handy, 1989; Warren & Hirth, 2006). In this study, we present new findings that provide additional constraints on the nature of weakening in a mantle shear zone.

GEOLOGICAL BACKGROUND

The Josephine Peridotite is the Jurassic-age mantle section of one of several coast range ophiolites, exposed in the westernmost belt of the Klamath Mountains, SW Oregon. It has experienced a well-documented history of deformation and melt-infiltration, which is manifested in a series of shear zones and tabular dunite and pyroxenite bodies (Dick, 1976, 1977; Loney & Himmelburg, 1976; Harding, 1988; Kelemen & Dick, 1995; Warren *et al.*, 2008). In the Fresno Bench area, all of the shear zones are steeply dipping, of dextral sense, and set in a comparatively weakly deformed harzburgite. Shear zones are identified in the field by two observations: the deflection of pre-existing pyroxenite layers and the development of millimeter-scale banding. The strike of the shear zone, together with the well-defined sense of shear and lineation, allows accurate measurements of the shear plane and shear direction. Deformation is inhomogeneous, with the magnitude of strain increasing from the margins to the center of the shear zone. The focus of this study is a shear zone that is less than 30 m wide. The core of the shear zone, which has a distinct microstructure described below, is less than 3 m wide.

METHODS

Oriented samples were collected along a transect approximately normal to the shear zone. For each sample, the orientation of nearby pyroxenite layers was measured. Shear strain was calculated from the deflection of this

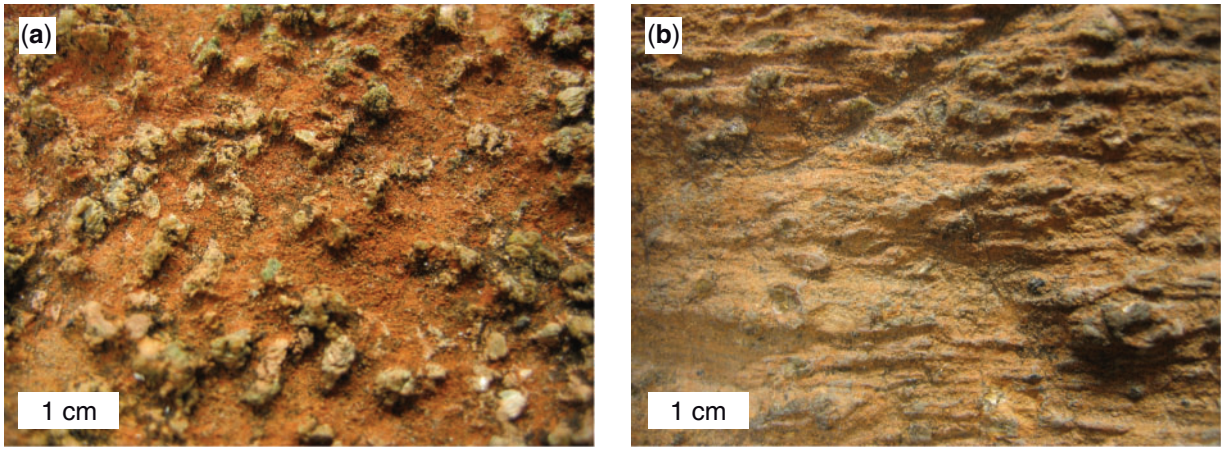

Fig. 2. Photographs of highly deformed and moderately deformed samples. (a) Sample 3925G08, from the margin of the shear zone. This sample is only moderately deformed, with blocky, unrecrystallized orthopyroxene grains. (b) Sample 3925G01, from the center of the shear zone. This sample is highly deformed, with fine-grained material forming millimeter-scale bands.

marker, following the technique of Warren *et al.* (2008). The orientation of the shear zone was measured in the field. Sampling extended from the center of the shear zone (where the maximum strain was achieved) to a point *c.* 15 m outside the shear zone where the orientation of pre-existing pyroxene layers is apparently unaffected by the shear zone. At the center of the shear zone, the pyroxene foliation and lineation become parallel to the shear plane (065/90) and the shear direction (34/065), respectively (Fig. 1).

Samples were reoriented in the laboratory, and thin-sections were cut with the long axis of the thin-section parallel to the shear direction, and the short axis of the thin-section normal to the shear plane. In most cases, several serial sections were prepared to ensure sufficient counting statistics in the subsequent analysis. Lattice-preferred orientation (LPO) of olivine and orthopyroxene was measured using electron backscatter-diffraction (EBSD) on a Philips XL30 FEG-SEM. An accelerating voltage of 20 kV and a beam current of 2.4 nA was used, at a working distance of 15–20 mm. The strength of the LPO was determined using the M-index technique (Skemer *et al.*, 2005). Chemical analyses were conducted using a Cameca SF-100 electron microprobe operating at 15 kV.

RESULTS

Microstructural observations

All samples studied have similar mineralogy consisting of olivine, orthopyroxene, spinel, and clinopyroxene. Clinopyroxene makes up less than 2% by volume, so these rocks are classified as harzburgites (Dick, 1977; Kelemen & Dick, 1995). There is some alteration (primarily serpentine and talc) along grain boundaries, particularly in fine-grained regions; however, this does not obscure the microstructure.

Based on the microstructures, the shear zone can be divided into two regions—a moderately deformed margin (Fig. 2a) and a highly deformed core (Fig. 2b). In the core of the shear zone, the accumulated strain is so large that the passive markers are essentially parallel to the shear plane. Therefore, we conservatively estimate the shear strain in the center of the shear zone to be greater than 20. The shear strain in the margin of the shear zone decreases with distance from the center, to a shear strain of 0·6 at a distance of 6·8 m from the center. The shear strain of sample JP08PS01, taken 15 m from the center of the shear zone, is assumed to be negligible during shear zone formation.

The moderately deformed samples from the margins of the shear zone have a homogeneous microstructure composed of mostly olivine and orthopyroxene (Fig. 3a and b). The grain size of both minerals is relatively coarse (2–3 mm) and the grains do not exhibit a strong shape-preferred orientation. There are occasional subgrain boundaries in both olivine and orthopyroxene, as well as evidence for grain-boundary migration. However, there is little evidence of grain-size reduction, in comparison with samples from the core of the shear zone.

The highly deformed samples from the core of the shear zone (Fig. 3c–f) exhibit two microstructural domains—relatively coarse-grained domains that contain only olivine (Fig. 3e), and finer-grained orthopyroxene-rich domains that contain mixtures of orthopyroxene, clinopyroxene, and olivine (Fig. 3f). Both the coarse- and fine-grained domains form laminar bands that are continuous on a thin-section scale (Fig. 3c and d).

Grain size was determined by the mean intercept technique, measuring 300–600 grains and applying a

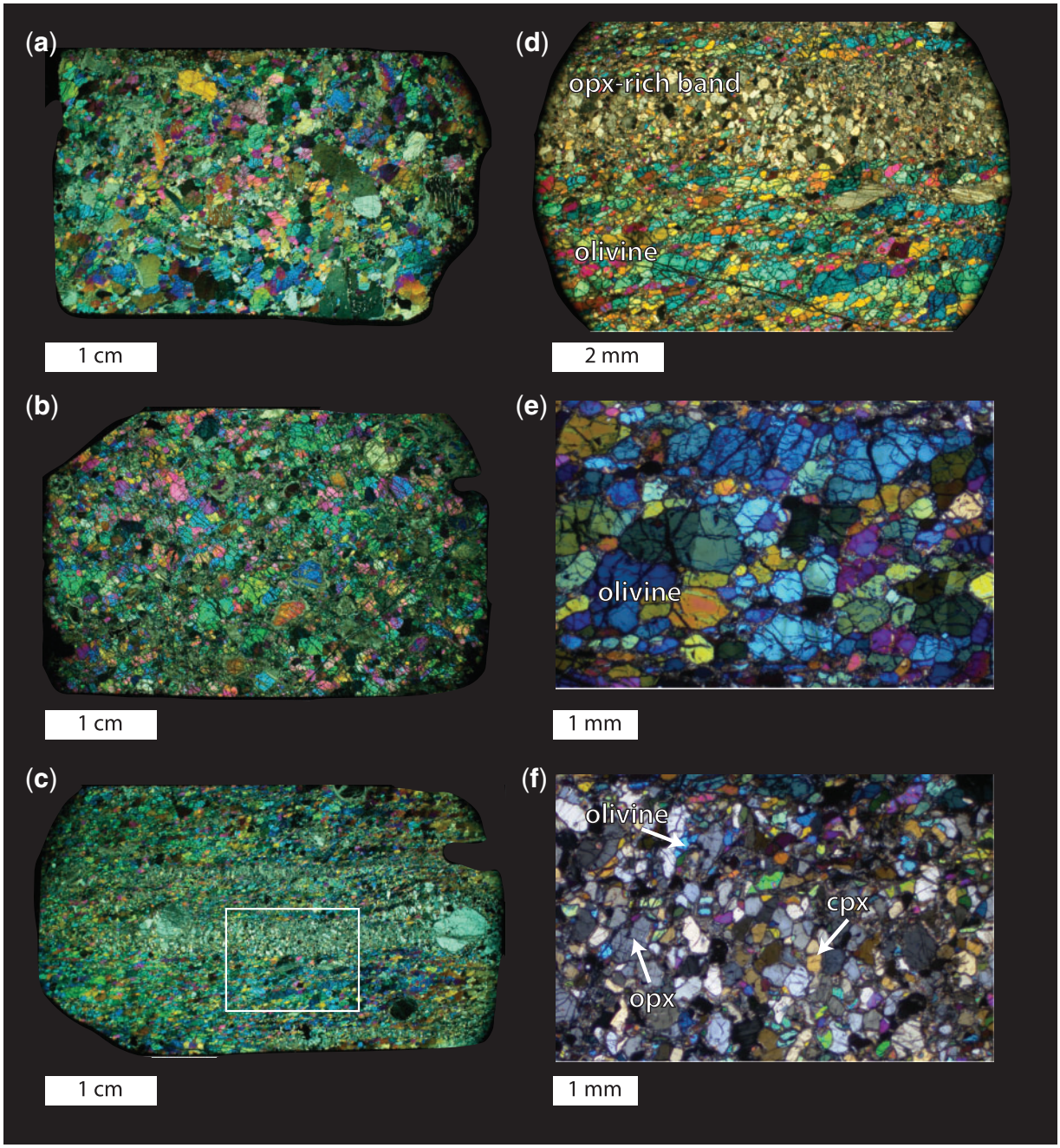

Fig. 3. Photomicrographs illustrating deformation microstructures in cross-polarized light. The long axes of the photomicrographs are parallel to the shear direction and the short axes are normal to the shear plane. The sense of shear in all figures is top to the right. (a) and (b) Moderately deformed samples (3925G08 and 3925G05, respectively) from the margin of the shear zone. These samples have a relatively simple microstructure composed of millimeter-scale olivine and orthopyroxene with only modest microstructural development. (c) A highly deformed sample from the core of the shear zone (3925G01). This sample has a well-developed microstructure with two distinct domains: relatively coarse-grained olivine regions and relatively fine-grained orthopyroxene-rich bands. (d) is an enlarged view of the outlined region in (c), illustrating both types of microstructures. (Note the oblique NE–SW-trending shape-preferred orientation in the coarse-grained olivine, which is coincident with the sense of shear.) (e) The relatively coarse-grained olivine-rich domain from the core of the shear zone (3925G01), showing stretched and internally deformed olivine grains. (f) The fine-grained orthopyroxene-rich domain from the core of the shear zone (3925G01), showing intimately mixed orthopyroxene and olivine, with little internal deformation and equant grain shapes.

Table 1: Microprobe analyses

	Orthopyroxene	Clinopyroxene
SiO_2	56·81	53·07
TiO_2	0·01	0·06
Al_2O_3	2·14	3·02
Cr_2O_3	0·56	1·00
FeO	5·68	2·38
MnO	0·13	0·08
MgO	34·03	17·68
CaO	0·94	23·03
Total	100·30	100·32

stereographic correction factor of 1·5. The grain size in the coarse olivine bands is ~550 μm whereas that in the fine-grained orthopyroxene rich domains is ~250 μm. Within the coarse-grained domain, the grains are somewhat elongated; clusters of grains with similar orientations indicate that dynamic recrystallization has occurred. The shape-preferred orientation of these grain clusters is coincident with the sense of shear (Fig. 3d). The similarity of extinction angles indicates that the sample has a strong lattice-preferred orientation; these optical effects are also consistent with LPO measurements made using EBSD. The fine-grained domains are intimately mixed, with varying proportions of olivine and orthopyroxene. Both olivine and orthopyroxene grains are largely equant. Fine-grained domains are generally associated with relict orthopyroxene porphyroclasts (Fig. 3c). There is no evidence of fracturing within the relict porphyroclasts, indicating that deformation was ductile. Many porphyroclasts have subgrain boundaries, indicating that their deformation was accommodated by dislocation creep.

Pyroxene thermometry

The temperature during deformation is estimated using the average compositions of adjacent pyroxene grains from within the fine-grained recrystallized domains in the core of the shear zone (Table 1). Applying the Brey & Koehler (1990) formulations for the two-pyroxene and Ca-in-opx thermometers we calculated temperatures of $980 \pm 25^{\circ}C$, assuming an equilibrium pressure of 1 GPa. This is in excellent agreement with previous results (Loney & Himmelburg, 1976; Harding, 1988).

Lattice-preferred orientation

All LPO data are plotted relative to a structural reference frame, where X is parallel to the shear direction and Z is normal to the shear plane. In the center of the shear zone, X is parallel to the orthopyroxene lineation and Z is normal to the orthopyroxene foliation. Orienting and cutting thin-sections and positioning the sample in the SEM are estimated to contribute no more than $\pm 5^{\circ}$ of uncertainty in the data. Samples 3925G01 and 3925G02, collected less than 1 m apart, give nearly identical results, providing confidence that data are reproducible. Some samples were also double checked on other EBSD systems, to ensure that the calibrations of both systems were accurate.

Within the shear zone margin, olivine *a*-axes are oriented at a moderate angle to the shear plane (Fig. 4, samples 3925G08, 3925G05, and 3925G04). With increasing deformation, the *a*-axes rotate towards the shear plane. However, unlike many previous observations (e.g. Zhang & Karato, 1995), the *a*-axes are clustered on the opposite side of the shear plane from the long axis of the finite strain ellipsoid (FSE). Olivine *c*-axes are clustered sub-normal to the shear plane, suggesting the operation of the [100] (001) slip system. Orthopyroxene fabrics are fairly weak in the margin of the shear zone; however, *c*-axis maxima are reasonably pronounced, and nearly aligned with the shear direction (samples 3925G08, 3925G05, and 3925G04).

Within the core of the shear zone the coarse-grained olivine-rich domain exhibits very strong LPOs ($M = 0{\cdot}37$–$0{\cdot}47$), with the *a*-axes sub-parallel to the shear direction and the *c*-axes sub-normal to the shear plane. Again, the *a*-axes are oriented on the opposite side of the shear plane from the long axis of the FSE. The obliquity of the LPO was confirmed in thin-section; the angle between the olivine extinction and the orthopyroxene foliation is the same as the rotation of the olivine LPO past the shear plane. This provides a good measure of confidence that the LPO measurements are accurate. In the fine-grained two-phase domains the symmetry of the olivine LPO is unchanged, although the strength of the fabric is weaker ($M = 0{\cdot}10$). In contrast to the margin of the shear zone, the fine-grained orthopyroxene does not exhibit a perceptible *c*-axis maxima; the LPO is essentially random, with $M < 0{\cdot}02$. Although the difference in the M-indices is modest, we also emphasize that the orientation of the weak *c*-axis maxima in this sample is not correlated with any kinematic indicator.

The sample furthest outside the shear zone has a similar LPO to the nominally undeformed sample of Warren *et al.* (2008), when plotted in the same geographical reference frame.

DISCUSSION

Interpretation of microstructures

Our data show considerable evidence for a microstructural and rheological transition in orthopyroxene with increasing strain. We have shown that in the shear zone margin orthopyroxene *c*-axes are generally aligned with the shear direction, indicating deformation by dislocation creep

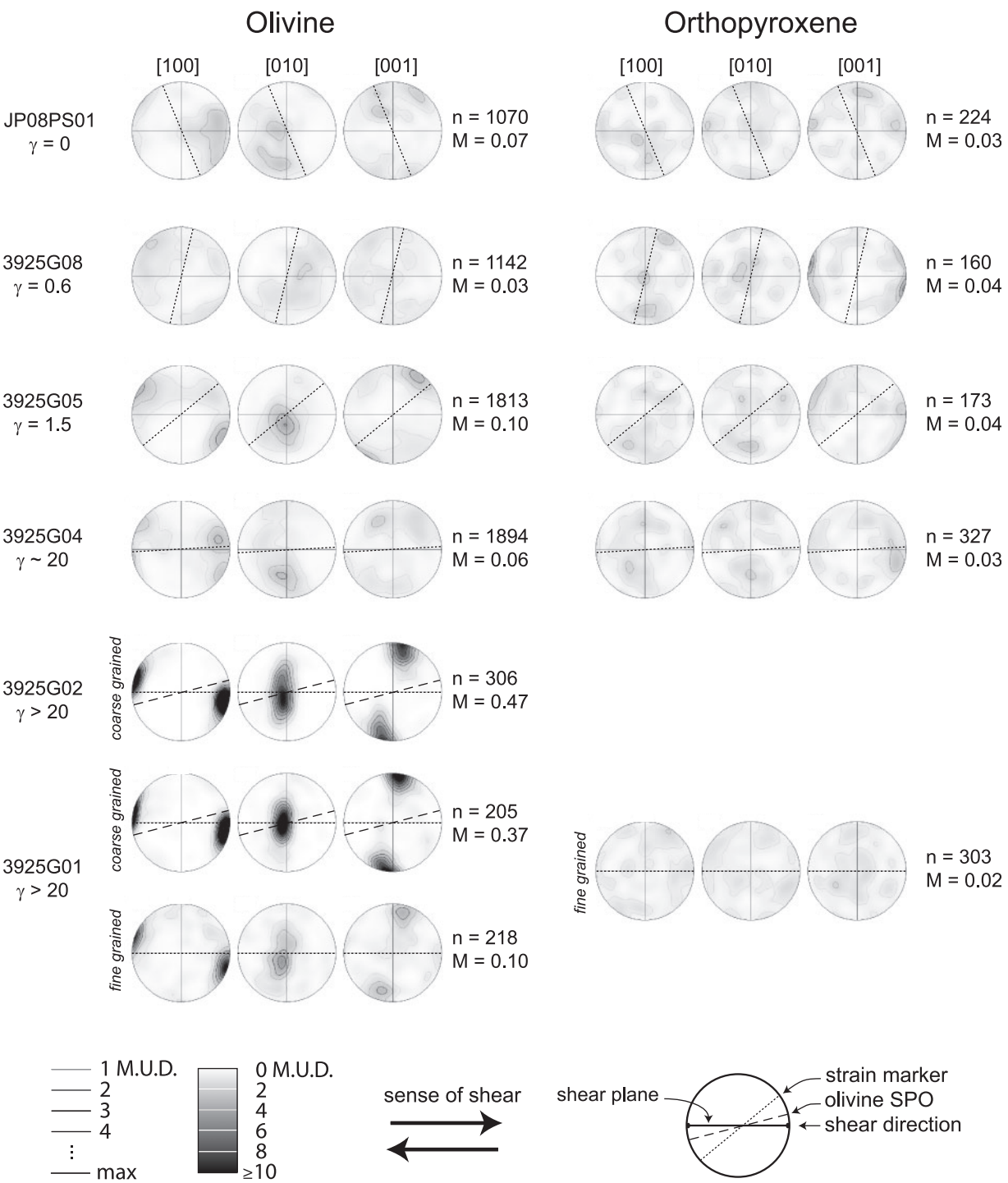

Fig. 4. Pole figures from all samples investigated in this study. Pole figures are upper hemisphere equal area projections, oriented with the shear direction east–west and the pole to the shear plane north–south. The sense of shear is top to the right. Dotted lines represent the orientations of the nearby pyroxenite bands, which are used as strain markers. Dashed lines show the orientation of the olivine shape-preferred orientation, when present. The contour interval is one multiple of uniform distribution (MUD). Shading saturates at 10 MUD. Data are smoothed with a 20° half-width Gaussian function. Samples are listed in increasing order of shear strain. Towards the center of the shear zone the pyroxene bands become parallel to the shear plane, so strain is only approximate. For each pole figure the number of data (n) and the M-index (M) are listed. All deformed olivine samples display E-type LPOs. In the shear zone margin orthopyroxene c-axes align with the shear direction. However, within the fine-grained band from the center of the shear zone, the orthopyroxene LPO is essentially random, and has no correlation with the imposed kinematics.

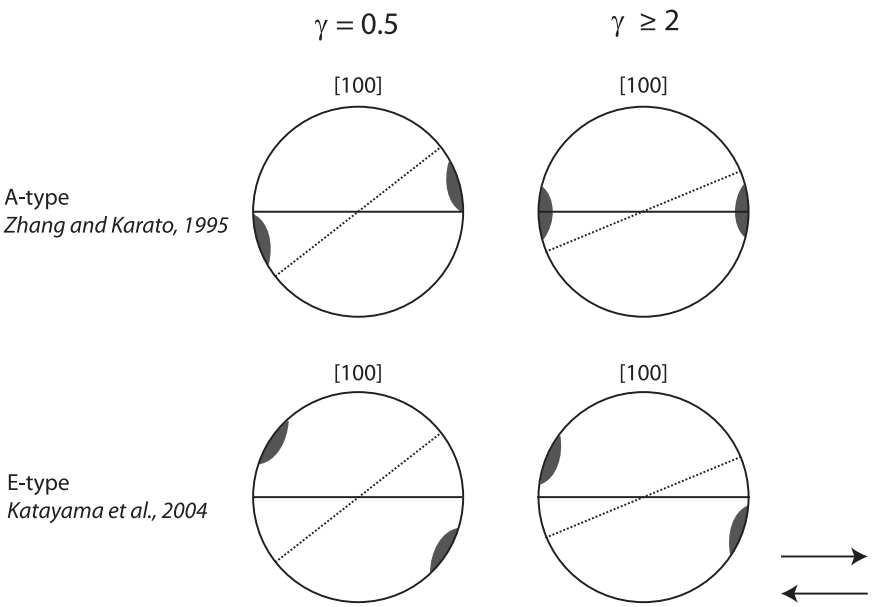

Fig. 5. Schematic diagram illustrating the rotation of olivine [100] maxima with strain for experimentally generated A- and E-type fabrics. Pole figures are oriented as in Fig. 4. Shaded regions represent locations of [100] maxima. The dotted lines show the orientation of the long axis of the finite strain ellipsoid (FSE) at shear strains of $\gamma = 0{\cdot}5$ (left) and $\gamma = 2$ (right). Data for A-type fabrics are from the experiments of Zhang & Karato (1995). Data for E-type fabrics are from the experiments of Katayama *et al.* (2004). In the experiments of Zhang & Karato (1995), the olivine [100] peak initially follows the long axis of the FSE, but rotates into the shear plane at relatively modest strains. In the experiments of Katayama *et al.* (2004) the [100] axes are oriented on the opposite side of the shear plane from the FSE. Although there is some rotation towards the shear plane, this oblique LPO pattern persists to shear strains of $\gamma = 6{\cdot}3$.

(e.g. Christensen & Lundquist, 1982). We have also shown that the recrystallized orthopyroxene from the core of the shear zone does not have an LPO. Moreover, the fine-grained bands display considerable intermixing of olivine and orthopyroxene. In highly deformed rocks such as these, the absence of LPO and evidence of grain switching (Ashby & Verrall, 1973) are generally correlated with the activity of a grain-size sensitive deformation mechanism (Fliervoet *et al.*, 1999; Warren & Hirth, 2006; Skemer & Karato, 2008). In addition, residual orthopyroxene porphyroclasts have equant dimensions, suggesting that they are no longer accommodating much deformation. Together, these observations suggest that after sufficient strain accumulation by dislocation creep, dynamic recrystallization produced bands of small recrystallized orthopyroxene neoblasts. Subsequent deformation of the orthopyroxene-rich bands apparently occurred in a grain-size sensitive regime, which may have resulted in a dramatic reduction in the strength of the rock as discussed below. Several researchers have identified similar rheological transitions in orthopyroxene in shear zones from the base of the lithosphere (Boullier & Gueguen, 1975; Skemer & Karato, 2008), to the shallower upper mantle (Dijkstra *et al.*, 2002), and to the lower crust (Raimbourg *et al.*, 2008).

All samples investigated in this study showed some evidence of olivine LPO. This suggests that deformation of olivine was predominantly accommodated by dislocation creep. In the more highly deformed samples, we see compelling evidence for the development of E-type LPOs, indicating that deformation took place in the presence of water (Katayama *et al.*, 2004). E-type fabrics have been identified in only a handful of naturally deformed rocks (Mehl *et al.*, 2003; Michibayashi & Mainprice, 2004; Sawaguchi, 2004). Our data are the first to identify E-type fabrics with respect to well-defined deformation kinematics.

The orientation of the olivine LPO, with the *a*-axis on the opposite side of the shear plane from the long axis of the FSE, is very similar to observations from experimentally generated E-type fabrics (Katayama *et al.*, 2004). Katayama *et al.* attributed the unusual nature of the E-type LPO to contributions from the complementary [001] (100) slip system. Given the large strains observed in this study, as well as in the laboratory experiments, we speculate that E-type fabrics may not fully rotate into concordance with the shear plane in most geological conditions. This is in notable contrast to observations of A-type fabrics, which rotate into the shear plane at relatively small strains (Zhang & Karato, 1995; Warren *et al.*, 2008). These scenarios are illustrated schematically in Fig. 5.

The observation of well-developed E-type fabrics in the Fresno Bench section of the Josephine peridotite provides new constraints on localization phenomena in the mantle. Studies of other mylonites in this area have found

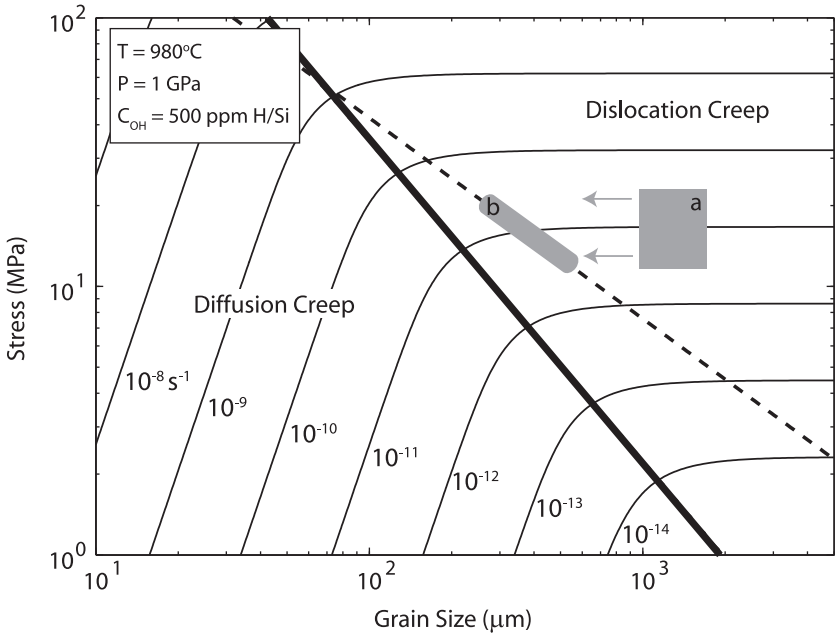

Fig. 6. Deformation mechanism map for olivine, calculated using flow laws from Hirth & Kohlstedt (2003). The bold line represents the boundary between dislocation creep dominated rheology and diffusion creep dominated rheology. The fine lines are contours of constant strain rate. The dashed line is the empirically calibrated grain-size piezometer from Karato *et al.* (1980) and van der Wal *et al.* (1993). The gray shaded rectangle labeled (a) shows the grain sizes and range of stresses for the margin of the shear zone, assuming stress is continuous across the shear zone. The gray shaded region labeled (b) shows the range of measured grain sizes and calculated stresses from the core of the shear zone. Even at these small grain sizes, diffusion creep plays only a minimal role in the accommodation of strain.

predominantly A- or D-type fabrics (Harding, 1988; Warren *et al.*, 2008), which are generated at dry conditions ($\leq \sim$200 H/10^6 Si in laboratory studies) (Jung & Karato, 2001; Katayama *et al.*, 2004). The localized observation of E-type fabrics suggests that the water required to generate the E-type LPO was also localized in the shear zone, either in space or in time. The source of the water is uncertain, but it may have been supplied by localized migration of fractionated melt before or during deformation. This is consistent with the hypothesis that these shear zones initiated along melt conduits (Kelemen & Dick, 1995). Preliminary analyses of Josephine rocks indicate that small amounts of water are still present (J. M. Warren, personal communication).

Estimating the conditions of deformation

The differential stress during deformation can be constrained from empirical grain-size or dislocation density piezometers. Typically, grain-size piezometers are more useful in natural systems, because dislocation microstructures are readily altered during subsequent deformation or exhumation. However, it is not strictly appropriate to apply an empirical grain-size piezometer to a poly-phase microstructure. The reason for this is that the relationship between grain size and stress is highly sensitive to grain boundary mobility (Derby & Ashby, 1987). The presence of secondary phases inhibits grain boundary motion (i.e. Zener pinning) (Evans *et al.*, 2001), which should result in a smaller recrystallized grain size for a given stress (Mehl & Hirth, 2008). As an additional complication, grain size may also be altered by post-deformation annealing. For a rough estimation of stress we will treat the olivine grain size within the fine-grained domain as an upper limit and the grain size within the coarse-grained domain as a lower limit, to account for pinning and static growth effects. Applying the piezometers of Karato *et al.* (1980) and van der Wal *et al.* (1993) we estimate a paleostress in the core of the shear zone of 13–20 MPa. The water content present during deformation is constrained by the olivine fabric type (Katayama *et al.*, 2004; Karato *et al.*, 2008). To generate an E-type fabrics, as found in this study, water contents in olivine must range from $\sim$200 to 1000 ppm H/Si. At the temperature determined by two-pyroxene thermometry (980°C), and assuming a melt-free rheology, this corresponds to strain rates of $\sim 4 \times 10^{-11}$ to 1×10^{-12} s^{-1} (Hirth & Kohlstedt, 2003). Given a conservative estimate of strain ($\gamma = 20$), these strain rates indicate that deformation could have occurred in as little as $\sim 10^4$ years. Although the diffusion of water is rapid in comparison with other chemical species (Mackwell & Kohlstedt, 1990), the time scale of deformation may have been short enough to maintain fairly high local concentrations of water.

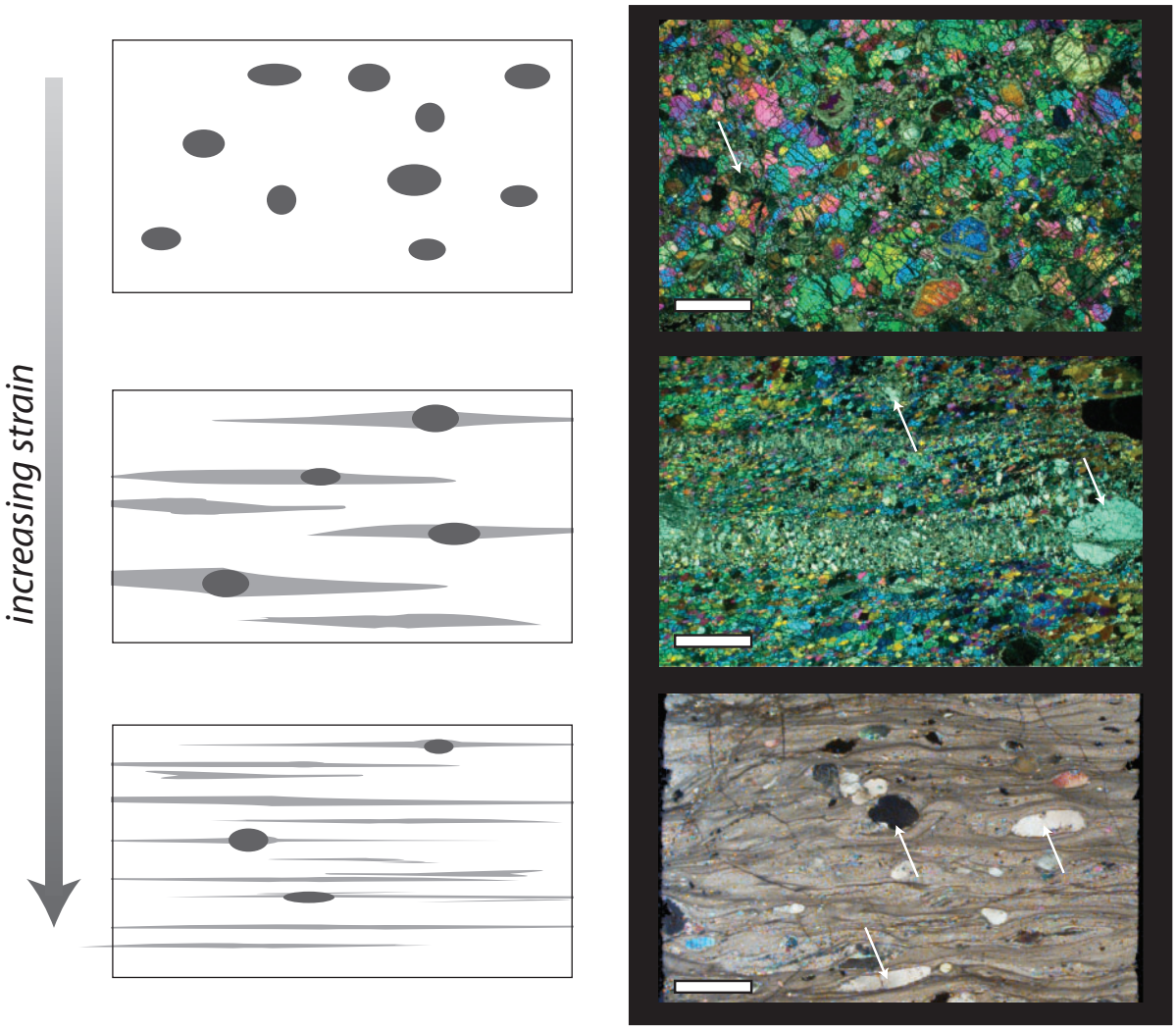

Fig. 7. Schematic model of microstructural evolution in peridotite mylonites. The drawings on the left show orthopyroxene (in gray) evolving from coarse-grained to fine-grained microstructures. Dark gray indicates orthopyroxene porphyroclasts and light gray indicates orthopyroxene-rich clusters of neoblasts. The photomicrographs on the right show examples of these microstructures (top: sample 3925G05, from this study; middle: sample 392G01, from this study; bottom: ultramylonite sample from Warren & Hirth, 2006). Scale bars in photomicrographs represent 5 mm. Some remnant orthopyroxene porphyroclasts are indicated by white arrows. In the middle and bottom panels, these orthopyroxene porphyroclasts are generally associated with bands of fine-grained recrystallized material.

At present, experimental data on the rheology of orthopyroxene are sparse, particularly in the diffusion creep regime and in the presence of water. However, the microstructures preserved in this shear zone provide some new constraints on the relative viscosity of olivine and orthopyroxene. Along the margins of the shear zone, the absence of flattening and recrystallization of orthopyroxene indicates that olivine accommodates much of the deformation. Within the highly deformed core of the shear zone, extrapolation of olivine flow laws suggests that most deformation is accommodated by dislocation creep (Fig. 6), which is consistent with the observation of strong LPO. However, a modest component of diffusion creep in the finer-grained domains may explain the difference in the strength of the olivine LPO between the coarse- and fine-grained domains in sample 3925G01. The absence of microboudinage textures in the most highly deformed rocks suggests that the domains of coarse-grained olivine have comparable viscosity to domains of fine-grained orthopyroxene–olivine mixtures. Thus, fine-grained orthopyroxene deforming by diffusion creep may not be significantly weaker than similarly fine-grained olivine deforming by dislocation creep.

A model of shear zone evolution

We suggest that the core of the shear zone experienced at least three stages of deformation, which may or may not have been temporally continuous. During the first stage,

homogeneous regional deformation produced a background microstructure in the sample. The microstructures in sample JP08PS01 from this study, and sample 3923J01 from Warren *et al.* (2008) reflect this stage of deformation. Although the magnitude of strain during this first stage of deformation is unknown, the conditions of deformation were insufficient to induce recrystallization in orthopyroxene. We assume that olivine, which forms a weak interconnected network, accommodated the majority of deformation. This hypothesis is supported qualitatively by the observation that olivine LPOs are better developed than orthopyroxene LPOs in these samples.

During a second stage of deformation, localization was initiated and the shear zone began to form. The precise mechanism for the initiation of localization is unclear. One possibility, which is consistent with the inferred presence of water during deformation, is that localization was initiated by the passage of melt through the host rock (Kelemen & Dick, 1995). The samples collected from the moderately deformed margin of the shear zone (3925G08, 3925G05, and 3925G04) reflect this second stage of deformation. Again, the orthopyroxene is largely unrecrystallized and probably played a minimal role in the aggregate rheology.

A third stage of deformation is characterized by the recrystallization of orthopyroxene. Significant macroscopic strain is required to reach this stage, because during the previous two stages strain was largely partitioned into the olivine. However, once significant recrystallization of orthopyroxene occurred, bands of fine-grained material were formed and rapidly became interconnected. Some sliding along olivine and orthopyroxene phase boundaries may have facilitated the intermixing of the two phases. During this third stage of deformation, strain was accommodated by both the coarse-grained olivine domains and the fine-grained olivine and orthopyroxene bands. We did not identify any samples with textures intermediate between stages two and three, indicating that this microstructural transition occurred over a fairly narrow length scale.

We speculate that the microstructures observed in this study represent an intermediate step between moderately deformed shear zones and highly deformed ultramylonites (Fig. 7). Moderately deformed shear zones (see Warren *et al.*, 2008), display localized deformation but do not exhibit any grain-size reduction. On the other end of the spectrum, highly deformed ultramylonites (see Drury *et al.*, 1991; Warren & Hirth, 2006) display extreme grain-size reduction and compositional banding, with an associated transition to grain-size sensitive deformation. In this study, the microstructures we observe contain elements of ultramylonite microstructures, although not developed to the same degree. Reactivation of a mylonite, of the type studied here, at higher stresses or lower temperatures, would probably result in a refinement of the microstructure to more closely resemble an ultramylonite. This suggests that we are observing what might be termed a proto-ultramylonite. The role of orthopyroxene is clearly important in mylonites, as it both inhibits grain growth and accommodates strain.

CONCLUSIONS

This study provides further evidence that large strain deformation will ultimately cause orthopyroxene to recrystallize, and that subsequent deformation may be in a rheologically weakened, grain-size sensitive state. Because of its intrinsic rheological behavior and its effect on olivine grain size, the recrystallization of orthopyroxene is an important mechanism for producing long-lived zones of weakness in the mantle lithosphere, and may therefore play an important role in the accommodation of plate tectonics. The E-type olivine fabrics identified in this study indicate that deformation took place in the presence of water. The observation that the [100] axes are rotated past the shear plane provides the first field-based confirmation of similar experimental observations. We speculate that the enhancement of localization in this shear zone, in comparison with the shear zone described by Warren *et al.* (2008), may be due to feedback between the intrusion of melt, the hydration of the surrounding rock, and the recrystallization and subsequent grain-size sensitive deformation of orthopyroxene.

ACKNOWLEDGEMENTS

This work was partly supported by NSF grants OCE-0452401 and EAR-0738880. Funding for fieldwork was provided by the WHOI Academic Programs Office (2003) and Columbia University (2006) as part of a field class run by P.B.K. and G.H. Comments by the editor, K. Michibayashi and an anonymous reviewer improved the wording and focus of the manuscript.

REFERENCES

Ashby, M. F. & Verrall, R. A. (1973). Diffusion-accommodated flow and superplasticity. *Acta Metallurgica* **21**, 149–163.

Bercovici, D. (2003). The generation of plate tectonics from mantle convection. *Earth and Planetary Science Letters* **205**, 107–121.

Bercovici, D. & Karato, S. i. (2002). Theoretical analysis of shear localization in the lithosphere. In: Karato, S. i. & Wenk, H. R. (eds) *Plastic Deformation of Minerals and Rocks*. Washington, DC: Mineralogical Society of America and Geochemical Society, pp. 387–420.

Boullier, A. M. & Gueguen, Y. (1975). SP-mylonites; origin of some mylonites by superplastic flow. *Contributions to Mineralogy and Petrology* **50**, 93–104.

Brey, G. P. & Koehler, T. (1990). Geothermobarometry in four-phase lherzolites; II, New thermobarometers, and practical assessment of existing thermobarometers. *Journal of Petrology* **31**, 1353–1378.

Christensen, N. I. & Lundquist, S. M. (1982). Pyroxene orientation within the upper mantle. *Geological Society of America Bulletin* **93**, 279–288.

Derby, B. & Ashby, M. (1987). On dynamic recrystallization. *Scripta Metallurgica* **21**, 879–884.

Dick, H. J. B. (1976). *The Origin and Emplacement of the Josephine Peridotite of Southwestern Oregon*. New Haven, CT: Yale University, 409 p.

Dick, H. J. B. (1977). Partial melting in the Josephine Peridotite I. Effect on mineral composition and its consequence for geobarometry and geothermometry. *American Journal of Science* **277**, 801–832.

Dijkstra, A. H., Drury, M. R., Vissers, R. L. M. & Newman, J. (2002). On the role of melt–rock reaction in mantle shear zone formation in the Othris Peridotite Massif (Greece). *Journal of Structural Geology* **24**, 1431–1450.

Drury, M. R., van der Vissers, R. L. M., van der Wal, D. & Hoogerduijn Strating, E. H. (1991). Shear localisation in upper mantle peridotites. *Pure and Applied Geophysics* **137**, 439–460.

Evans, B., Renner, J. & Hirth, G. (2001). A few remarks on the kinetics of static grain growth in rocks. In: Dresen, G. & Handy, (eds) *Deformation Mechanisms, Rheology and Microstructures*. Berlin: Springer, pp. 88–103.

Fliervoet, T. F., Drury, M. R. & Chopra, P. N. (1999). Crystallographic preferred orientations and misorientations in some olivine rocks deformed by diffusion or dislocation creep. In: Schmid, S. M., Heilbronner, R. & Stuenitz, H. (eds) *Deformation Mechanisms in Nature and Experiment*. Amsterdam: Elsevier, pp. 1–27.

Handy, M. R. (1989). Deformation regimes and the rheological evolution of fault zones in the lithosphere; the effects of pressure, temperature, grainsize and time. *Tectonophysics* **163**, 119–152.

Harding, D. (1988). *Josephine Peridotite Tectonites: A Record of Upper-mantle Plastic Flow*. Ithaca, NY: Cornell University, 334 p.

Hirth, G. & Kohlstedt, D. L. (2003). Rheology of the upper mantle and the mantle wedge: A view from the experimentalists. In: Eiler, J. (ed.) *Inside the Subduction Factory. American Geophysical Union, Geophysical Monograph* **138**, 83–105.

Jung, H. & Karato, S.i. (2001). Water-induced fabric transitions in olivine. *Science* **293**, 1460–1462.

Karato, S. i., Toriumi, M. & Fujii, T. (1980). Dynamic recrystallization of olivine single crystals during high-temperature creep. *Geophysical Research Letters* **7**, 649–652.

Karato, S.-i., Jung, H., Katayama, I. & Skemer, P. (2008). Geodynamic significance of seismic anisotropy of the upper mantle: New insights from laboratory studies. *Annual Review of Earth and Planetary Sciences* **36**, 59–95.

Katayama, I., Jung, H. & Karato, (2004). New type of olivine fabric from deformation experiments at modest water content and low stress. *Geology (Boulder)* **32**, 1045–1048.

Kelemen, P. & Dick, H. (1995). Focused melt flow and localized deformation in the upper mantle: Juxtaposition of replacive dunite and ductile shear zones in the Josephine peridotite, SW Oregon. *Journal of Geophysical Research* **100**, 423–438.

Loney, R. A. & Himmelburg, G. R. (1976). Structure of the Vulcan Peak alpine-type peridotite, southwestern Oregon. *Geological Society of America Bulletin* **87**, 259–274.

Mackwell, S. J. & Kohlstedt, D. L. (1990). Diffusion of hydrogen in olivine; implications for water in the mantle. *Journal of Geophysical Research, B, Solid Earth and Planets* **95**, 5079–5088.

Mehl, L. & Hirth, G. (2008). Plagioclase preferred orientation in layered mylonites: Evaluation of flow laws for the lower crust. *Journal of Geophysical Research—Solid Earth* **113**, 19.

Mehl, L., Hacker, B. R., Hirth, G. & Kelemen, P. B. (2003). Arc-parallel flow within the mantle wedge: Evidence from the accreted Talkeetna arc, south central Alaska. *Journal of Geophysical Research* **108**, 4-1–4-18.

Michibayashi, K. & Mainprice, D. (2004). The role of pre-existing mechanical anisotropy on shear zone development within oceanic mantle lithosphere: An example from the Oman ophiolite. *Journal of Petrology* **45**, 405–414.

Newman, J., Lamb, W. M., Drury, M. R. & Vissers, R. L. M. (1999). Deformation processes in a peridotite shear zone: reaction-softening by an H_2O-deficient, continuous net transfer reaction. *Tectonophysics* **303**, 193–222.

Raimbourg, H., Toyoshima, T., Harima, Y. & Kimura, G. (2008). Grain-size reduction mechanisms and rheological consequences in high-temperature gabbro mylonites of Hidaka, Japan. *Earth and Planetary Science Letters* **267**, 637–653.

Rutter, E. H. & Brodie, K. H. (1988). The role of tectonic grain size reduction in the rheological stratification of the lithosphere. In: Zankl, H., Belliere, J. & Prashnowsky, A. (eds) *Detachment and Shear*. Berlin: Springer, pp. 295–308.

Sawaguchi, T. (2004). Deformation history and exhumation process of the Horoman Peridotite Complex, Hokkaido, Japan. *Tectonophysics* **379**, 109–126.

Skemer, P. & Karato, S. (2008). Sheared lherzolite xenoliths revisited. *Journal of Geophysical Research* **113**, B07205.

Skemer, P., Katayama, I., Jiang, Z. & Karato, S.-i. (2005). The misorientation index: Development of a new method for calculating the strength of lattice-preferred orientation. *Tectonophysics* **411**, 157–167.

van der Wal, D., Chopra, P., Drury, M. & Fitz, G. J. (1993). Relationships between dynamically recrystallized grain size and deformation conditions in experimentally deformed olivine rocks. *Geophysical Research Letters* **20**, 1479–1482.

Vissers, R. L. M., Drury, M. R., Newman, J. & Fliervoet, T. F. (1997). Mylonitic deformation in upper mantle peridotites of the North Pyrenean Zone (France): implications for strength and strain localization in the lithosphere. *Tectonophysics* **279**, 303–325.

Warren, J. M. & Hirth, G. (2006). Grain size sensitive deformation mechanisms in naturally deformed peridotites. *Earth and Planetary Science Letters* **248**, 438–450.

Warren, J. M., Hirth, G. & Kelemen, P. (2008). Evolution of lattice-preferred orientation during simple shear in the mantle. *Earth and Planetary Science Letters* **272**, 501–512.

White, S. H., Burrows, S. E., Carreras, J., Shaw, N. D. & Humphreys, F. J. (1980). On mylonites in ductile shear zones. In: Carreras, J., Cobbold, P. R., Ramsay, J. G. & White, S. H. (eds) *Shear Zones in Rocks*. Oxford: Pergamon Press, pp. 175–187.

Zhang, S. & Karato, (1995). Lattice preferred orientation of olivine aggregates deformed in simple shear. *Nature* **375**, 774–777.